Microtubule-Dependent Movement of Late Endocytic Vesicles In Vitro: Requirements for Dynein and Kinesin

Eustratios Bananis,*† Sangeeta Nath,*† Kristie Gordon,‡ Peter Satir,*†
Richard J. Stockert,* John W. Murray,*† and Allan W. Wolkoff*†§

*Marion Bessin Liver Research Center, †Department of Anatomy and Structural Biology, and ‡Fluorescence Activated Cell Sorting Facility, Albert Einstein College of Medicine, Bronx, New York 10461

Our previous studies demonstrated that fluorescent early endocytic vesicles prepared from rat liver after injection of Texas red asialoorosomucoid contain asialoglycoprotein and its receptor and move and undergo fission along microtubules using kinesin I and KIFC2, with Rab4 regulating KIFC2 activity (J. Cell Sci. *116*, 2749, 2003). In the current study, procedures to prepare fluorescent late endocytic vesicles were devised. In addition, flow cytometry was utilized to prepare highly purified fluorescent endocytic vesicles, permitting validation of microscopy-based experiments as well as direct biochemical analysis. These studies revealed that late vesicles bound to and moved along microtubules, but in contrast to early vesicles, did not undergo fission. As compared with early vesicles, late vesicles had reduced association with receptor, Rab4, and kinesin I but were highly associated with dynein, Rab7, dynactin, and KIF3A. Dynein and KIF3A antibodies inhibited late vesicle motility, whereas kinesin I and KIFC2 antibodies had no effect. Dynamitin antibodies prevented the association of late vesicles with microtubules. These results indicate that acquisition and exchange of specific motor and regulatory proteins characterizes and may regulate the transition of early to late endocytic vesicles. Flow cytometric purification should ultimately facilitate detailed proteomic analysis and mapping of endocytic vesicle-associated proteins.

INTRODUCTION

Receptor-mediated endocytosis is a process in which the binding of a ligand to a specific cell surface receptor initiates an intricate series of events resulting in internalization of the ligand-receptor complex into a vesicle that is processed to discrete destinations within the cell. In the case of ligands such as asialoorosomucoid (ASOR), after its dissociation from receptor, the vesicle undergoes fission into daughter vesicles that deliver ligand to lysosomes for degradation and receptor to the cell surface where it is reutilized (Wolkoff et al., 1984; Mellman, 1996; Mukherjee et al., 1997; Murray and Wolkoff, 2003). Our earlier studies have shown an important role of the microtubule (MT)-based cytoskeleton in this process (Wolkoff et al., 1984; Oda et al., 1995; Novikoff et al., 1996). More recently we have reconstituted motility, fission, G-protein interactions, and ligand-receptor segregation of hepatocyte-derived early endocytic vesicles in an in vitro system in which microtubules have been attached to the surface of glass microscopy chambers (Murray et al., 2002; Murray et al., 2000; Bananis et al., 2000; Bananis et al., 2003). This report extends these studies to characterization of late, postsegregation, ligand-containing endocytic vesicles and presents evidence that changes in motor and scaffold pro-

teins occur on the endocytic vesicle as it progresses from pre- to postsegregation states.

These experiments utilize reagents that we have developed for studies of the hepatocyte specific asialoglycoprotein receptor (ASGPR) and its prototypical ligand, ASOR (Stockert, 1995). In previous investigations, fluorescent early endocytic vesicles were prepared from rat livers 5 min after injection of fluorescently labeled ASOR (Bananis et al., 2000; Bananis et al., 2003). Both ligand and receptor were colocalized in these vesicles, and individual vesicles moved with equal probability toward the plus and minus ends of MTs. These vesicles were associated with a classical plus-end–directed kinesin, but inhibitor and antibody studies showed that the minus-end motor on the vesicles was not cytoplasmic dynein as we (Oda et al., 1995) and others (Aniento et al., 1993; Pol et al., 1997) anticipated, but rather KIFC2, a minus-end–directed kinesin. Rab4-GTP was bound to these vesicles and its conversion to Rab4-GDP was associated with increased KIFC2-mediated minus-end–directed motility and vesicle fission (Bananis et al., 2003).

In the present investigation, late endocytic vesicles were prepared from rat livers 15 min after injection of fluorescently labeled ASOR. We show that these vesicles have little association with ASGPR or Rab4 but are highly associated with dynein, KIF3A, and Rab7. We demonstrate that MT-based motility of these vesicles is mediated by dynein and KIF3A, with which they interact via the dynactin complex. Additionally, we have devised flow cytometry–based methodology to purify fluorescent ligand-containing early and late endocytic vesicles. This has enabled biochemical analysis that validates results obtained using fluorescence micros-

copy of mixed vesicle populations. Altogether, these studies indicate that during maturation and movement along MTs toward lysosomes, endocytic vesicles acquire and exchange specific motor, regulatory, and scaffold proteins. The mechanism by which this occurs remains to be elucidated, but may regulate the transition of early to late endocytic vesicles.

MATERIALS AND METHODS

Chemicals and Reagents

ASOR was prepared from human orosomucoid (Sigma, St. Louis, MO) by acid hydrolysis (Stockert *et al.*, 1980). Mouse IgG monoclonal antibodies against the dynein intermediate chain (IC) and the kinesin I heavy chain (HC) were obtained from Chemicon International (Temecula, CA). Affinity-purified rabbit IgGs against the dynein heavy chain (HC) and Rab7 were purchased from Santa Cruz Biotechnology (Santa Cruz, CA). Rabbit antiserum against KIF5B was kindly provided by Dr. Larry Goldstein (UCSD, LaJolla, CA). Affinity-purified rabbit IgG against KIFC2 was purchased from Affinity Bioreagents (Golden, CO). Affinity-purified rabbit IgG was prepared against a KLH-linked peptide (VNRWACERKRDITYC) corresponding to a sequence on the cytoplasmic tail of the rat asialoglycoprotein receptor (ASGPR). Mouse monoclonal antibodies against Rab4, Rab5, dynactin p50, p150^{Glued} (dynactin), and KIF3A were obtained from BD Biosciences (Transduction Laboratories, San Diego, CA). Mouse IgG mAb against kinesin II was purchased from Babco (Richmond, CA). All fluorescent secondary antibodies were purchased from Jackson ImmunoResearch (West Grove, PA). Tubulin was purchased from Cytoskeleton (Denver, CO). All other reagents were from Sigma unless otherwise noted.

Endocytic Vesicle Isolation and Motility Assay

ASOR was labeled with Texas red sulfonyl chloride or Alexa Fluor 488 carboxylic acid, succinimidyl ester (Molecular Probes, Eugene, OR) according to the manufacturer's protocols. Fluorescent early and late endocytic vesicles were prepared from livers that that were removed from 200–250-g male Sprague Dawley rats (Taconic Farms, Germantown, NY) at 5 or 15 min after portal venous injection of 50 µg of fluorescently labeled ASOR, respectively (Murray *et al.*, 2000; Bananis *et al.*, 2000, 2003). All animal procedures were approved by the University Animal Use Committee. After Dounce homogenization, a postnuclear supernatant was prepared and chromatographed on a Sephacryl S200 column. Vesicle-enriched peaks were pooled and subjected to centrifugation (200,000 × *g* for 135 min) on a sucrose step gradient consisting of 1.4, 1.2, and 0.25 M sucrose. Vesicles were harvested from the 1.2 M/0.25 M sucrose interface and stored at −80°C until used. Details of these procedures have been published previously (Murray *et al.*, 2000). Two to three endocytic vesicle isolations per time point were used for the experiments.

Motility assays were performed in a chamber consisting of two pieces of double-sided tape sandwiched between optical glass; the internal volume was ~3 µl. The chamber was coated with 0.02 mg/ml DEAE-dextran (Amersham Pharmacia Biotech, Piscataway, NJ) and rhodamine-labeled, taxol-stabilized microtubules (MTs) were added and incubated for 3 min (Bananis *et al.*, 2000, 2003). After three washes with PMEE motility buffer (35 mM Pipes-K$_2$, 5 mM MgCl$_2$, 1 mM EGTA, 0.5 mM EDTA, 4 mM DTT, 20 µM Taxol, 2 mg/ml BSA, pH 7.4, containing an oxygen-scavenging system) containing 5 mg/ml casein, endocytic vesicles were added to the chamber, incubated for 10 min, and washed. Motility was initiated by the addition of 50 µM ATP in the absence of a regenerating system and sometimes in the presence or absence of 5 µM vanadate or 1 mM AMP-PNP. In some experiments, polarity-marked, rhodamine-labeled microtubules were prepared to determine directionality of moving Texas-Red-ASOR vesicles (Murray *et al.*, 2000). In other experiments, MT-bound vesicles were incubated with 4 mM guanine nucleotide analogues or antibodies against specific motor proteins for 6 min at room temperature, before ATP addition using methods that we have described previously (Bananis *et al.*, 2003).

Immunofluorescence Studies

These studies were performed as we have described previously (Murray *et al.*, 2002; Bananis *et al.*, 2000, 2003). In brief, primary antibodies diluted as appropriate in 5 mg/ml casein-containing PMEE buffer were perfused through the motility chamber containing MT-bound vesicles, incubated for 6 min at room temperature, and blocked with motility buffer containing 5 mg/ml casein. Cy2-labeled affinity-purified secondary antibody was added and incubation was continued for an additional 6 min. After extensive washing with PMEE buffer containing 5 mg/ml casein, immunofluorescence microscopy was performed. In some experiments, early and/or late endocytic vesicles were incubated with mAb against dynactin p50 (dynamitin) and/or nonimmune mouse IgG (62.5 ng/µl final concentration, respectively) for 5 min at 4°C before attachment to microtubules. Colocalization of MT-bound ASOR-containing vesicles with antibodies to candidate proteins was deter-
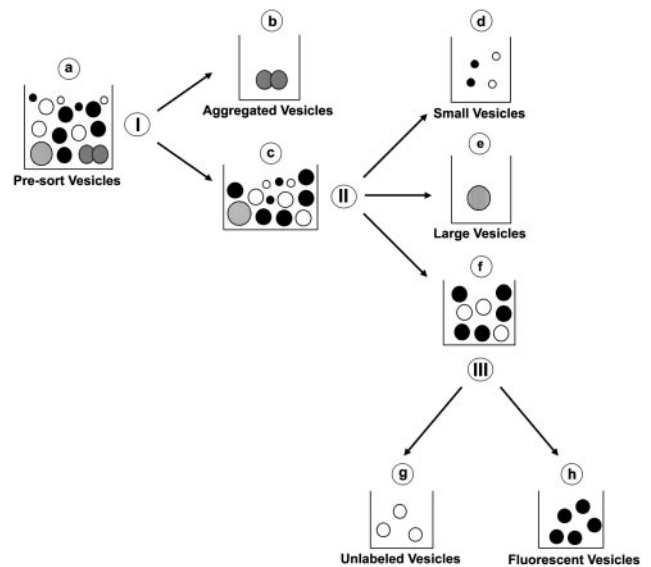

Figure 1. Schematic diagram of the flow cytometric purification of fluorescent endocytic vesicles. Presorted vesicles (a) were assessed from the dot plot representation of forward scatter (FSC) and pulse width (I) and set on a linear scale. Approximately, 90–95% of these vesicles (c) were gated and assessed for forward (FSC) and side scatter (SSC; II) set on a linear scale. From this, ~95% of vesicles (f) were gated for fluorescence analysis (III).

mined by first quantifying in the red channel the total number of bright fluorescent vesicles bound to dimmer labeled linear MTs. Subsequently the green channel was overlaid to quantify ligand-containing vesicles that colocalized with antibodies to specific proteins.

Image Analysis

Imaging was performed at the Analytical Imaging Facility of the Albert Einstein College of Medicine. A 60×, 1.4 NA planapo objective was used on an Olympus 1 × 70 inverted microscope containing automatic excitation and emission filter wheels connected to a Photometrics charge-coupled device camera run by IPLab Spectrum software (Scanalytics, Fairfax, VA) running on a Power Macintosh (Apple Computer, Inc, Cupertino, CA). IPLab Spectrum scripting software was used to collect images rapidly and to switch between fluorescence channels. Images were also recorded directly onto videotape. In all experiments the microscope stage was maintained at 35°C. Videos were digitized with the use of the Scion Image (Scion Corporation, Frederick, MD) movie-making macro (1 frame/s) and saved as tiff files. Corresponding frames indicating the staining in the different fluorescence channels were merged using Adobe Photoshop v. 6.0 (San Jose, CA).

Flow Cytometric Purification of Fluorescent Early and Late Endocytic Vesicles

Alexa 488–labeled endocytic vesicles were analyzed and sorted on a Dako-Cytomation Modular Flow (MoFlo) High-Performance Cell Sorter (DakoCytomation Inc., Fort Collins, CO) equipped with a 488-nm Coherent argon laser and a collection/emission 530/40-nm filter. Unlabeled vesicles were isolated from rat livers without prior injection of ASOR and used as controls. Data acquisition and analysis was performed using DakoCytomation MoFlo Summit Software (DakoCytomation Inc.). A flow diagram indicating the parameters used simultaneously to analyze and purify fluorescent vesicles and other subpopulations of vesicles is shown in Figure 1. Presorted vesicles (a) were assessed from the dot plot representation of forward scatter (FSC) and pulse width (I) and set on a linear scale (doublet discrimination parameter). Doublet discrimination allows for the identification of events that are actually two events bound together or two events that traverse the laser beam coincidentally. These "doublet" events can be eliminated from the sort and therefore ensure purity of the sorted population (Wersto *et al.*, 2001). Approximately 90–95% of these vesicles (c) were gated and assessed for forward (FSC) and side scatter (SSC; II) set on a linear scale (size discrimination parameter). From this, ~95% of vesicles (f) were gated for fluorescence analysis (III). A histogram plot on a log scale was created to determine the fluorescence intensity of unlabeled (g) or fluorescent vesicles (h). In some experiments, vesicles that did not meet sorting criteria and would have been discarded because of size discrimination parameters were collected and an-
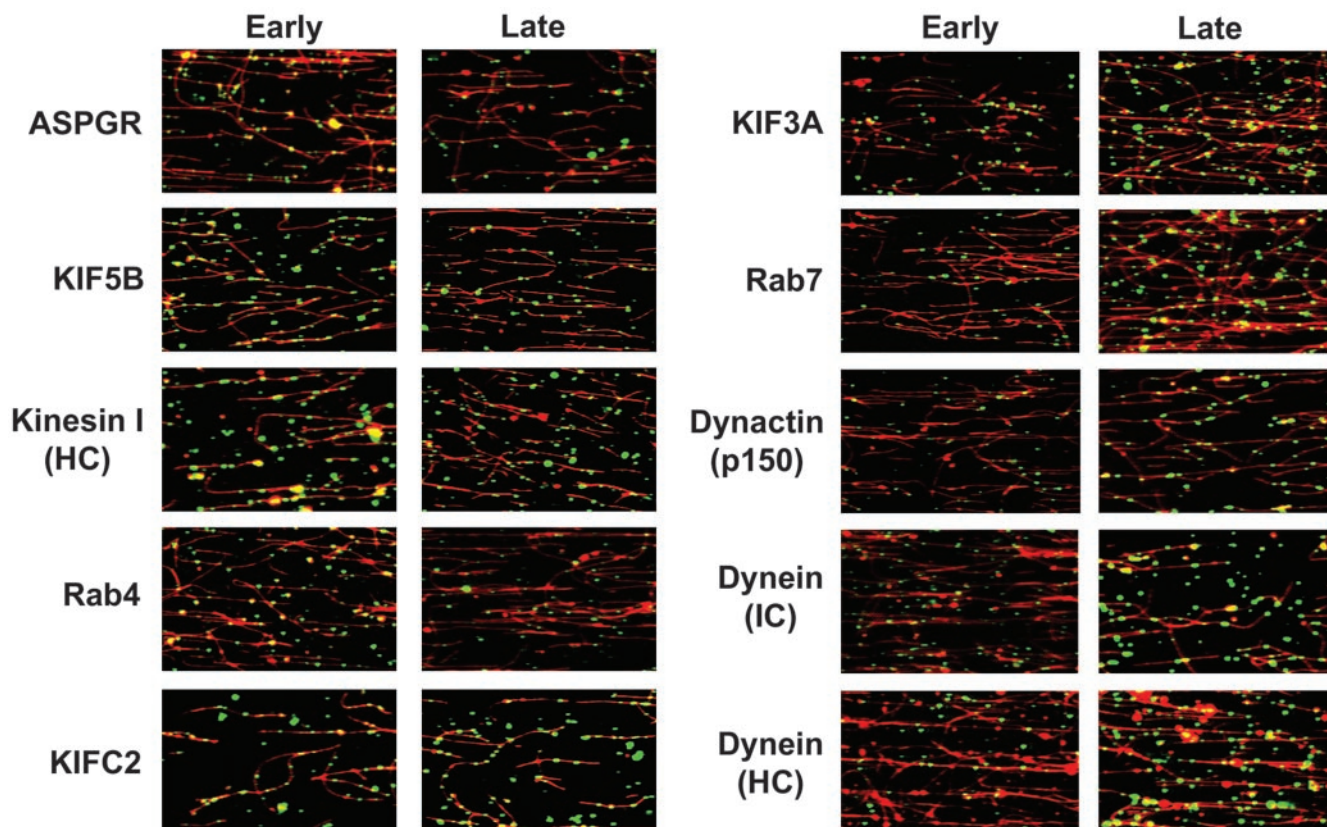
Figure 2. Immunofluorescence detection of endocytic vesicle-associated proteins. Texas-red–labeled ASOR-containing early (left panels) or late (right panels) endocytic vesicles were bound to rhodamine-labeled taxol-stabilized MTs. MT-bound vesicles were incubated for 6 min with primary antibodies against the indicated proteins, followed by addition of appropriate Cy2-labeled secondary antibodies (green). Corresponding images from both channels were merged. Colocalization between vesicles and proteins results in yellow vesicles. These studies indicate that early vesicles associate with ASGPR (receptor), conventional kinesin I (KIF5B, kinesin I [HC]), Rab4 and KIFC2, whereas late vesicles associate with KIFC2, KIF3A (kinesin II), Rab7, dynein, and dynactin (p150). MT-bound vesicles that do not contain fluorescent ligand are also seen associated with these proteins. HC, heavy chain; IC, intermediate chain.

alyzed. These vesicles included those of unusually large size (e) and aggregates (b). In addition, vesicles that were below the size detection limit of the flow cytometer (termed small vesicles; d) and were discarded during the sorting procedure were also collected and analyzed.

In similar experiments, before flow cytometry analysis, vesicles (a) were labeled with the general membrane marker Vybrant DiD cell-labeling solution (Molecular Probes) according to the manufacturer's protocol. Free dye was removed using MicroBio-spin P-30 columns (Bio-Rad Laboratories, Hercules, CA). Mixed (f) and fluorescence sorted (g and h) vesicles were analyzed for DiD-membrane and Alexa 488–ASOR fluorescence to assess colocalization of these two fluors.

Immunoblot Analysis

Vesicles collected via flow cytometry were centrifuged at 55,000 rpm for 75 min at 4°C in a Beckman TLA-100 centrifuge (Palo Alto, CA). Protein concentrations of pellets were determined by BCA assays (Bio-Rad Laboratories). Approximately 8 μg total protein was subjected to 10–20% gradient SDS-PAGE under reducing conditions. After transfer to nitrocellulose, the blot was blocked in TBS containing 0.1% Tween 20 and 10% nonfat dried milk. Immunoblot analysis was then performed using appropriate primary and HRP-conjugated secondary antibodies as described previously (Bananis *et al.,* 2003).

Statistical Analysis

Statistical analysis was performed using Chi-square or Student's *t* tests as appropriate (SigmaStat v 2.0, SPSS, Chicago, IL).

RESULTS

Identification of Proteins Associated with Late Endocytic Vesicles

To identify and contrast motor and accessory proteins that are associated with preparations of early and late endocytic vesicles, immunofluorescence microscopy was performed using a panel of antibodies to candidate proteins. Representative fluorescence images are shown in Figure 2, and quantitation of the fraction of Texas red-ASOR–containing vesicles that colocalize with a specific antibody is shown in Figure 3. In agreement with our previous studies (Bananis *et al.,* 2000, 2003), early endocytic vesicles have substantial association with the asialoglycoprotein receptor (ASGPR), conventional kinesin I (KIF5B and kinesin I), Rab4, and KIFC2. They have little association with KIF3A (kinesin II), Rab7, dynactin, or dynein. In contrast, few late endocytic vesicles were associated with the ASGPR, conventional kinesin I, or Rab4, but were highly associated with KIF3A, Rab7, KIFC2, dynactin, and dynein. Lack of association with the ASGPR is consistent with their assignment as postsegregation endocytic vesicles; i.e., they contain ligand but not receptor.
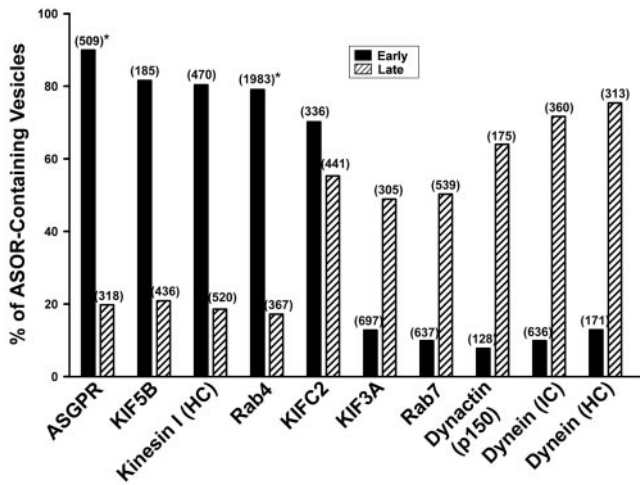
Figure 3. Quantitation of endocytic vesicle associated proteins as determined by immunofluorescence. Quantitation of colocalization studies as in Figure 2, was performed as described in MATERIALS AND METHODS. The total number of MT-bound early and late vesicles examined is shown in parentheses. Asterisk indicates published data (Bananis *et al.,* 2003).

Microtubule-based Motility of Late Endocytic Vesicles

Of the MT-bound early and late ASOR-containing vesicles, 23 and 26% of each population, respectively, moved upon addition of 50 μM ATP (Figure 4A). Few late, compared with early, endocytic vesicles underwent fission (Figure 4B). Our earlier studies indicated that motility and fission of early endocytic vesicles were markedly reduced after pretreatment with 1 mM AMP-PNP, but not 5 μM vanadate (Bananis *et al.,* 2000). At these concentrations, AMP-PNP inhibits activity of kinesins (Vale *et al.,* 1992; Fullerton *et al.,* 1998), whereas vanadate inhibits activity of dynein (Kobayashi *et al.,* 1978). In contrast, both agents substantially reduced the number of motile late endocytic vesicles (Figure 5), even in the presence of as much as 4 mM ATP (unpublished data). Early endocytic vesicles moved toward the plus and minus ends of polarity-marked microtubules equally well (Figure 6), confirming our earlier results (Bananis *et al.,* 2000). Minus-end–directed movement of late endocytic vesicles was substantially reduced by vanadate (Figure 6), suggesting that dynein mediated the minus-end–directed motility of late, but not early, endocytic vesicles. In previous studies (Bananis *et al.,* 2003) we found that pretreatment of early endocytic vesicles with GDP enhanced motility and fission, whereas pretreatment with GTP-γ-S was inhibitory. These effects were related to the guanosine nucleotide state of Rab4. In contrast to these results, pretreatment of late endocytic vesicles with GDP or GTP-γ-S did not alter their motility or fission (Table 1).

Effects of Antibodies to Motors and Motor Complexes on Motility of Late Endocytic Vesicles

Previous studies revealed that antibodies to kinesin I and KIFC2 inhibited motility and fission of early endocytic vesicles (Bananis *et al.,* 2000, 2003). In contrast, as seen in Figure 7, these antibodies had no effect on the motility of late endocytic vesicles. However, antibodies to KIF3A and cytoplasmic dynein substantially reduced late endocytic vesicle motility (Figure 7). Dynein is known to interact with its cargo through the dynactin complex and dynamitin (a p50 subunit of the dynactin complex) overexpression disrupts this complex resulting in inhibition of dynein-mediated motility (Karki and Holzbaur,
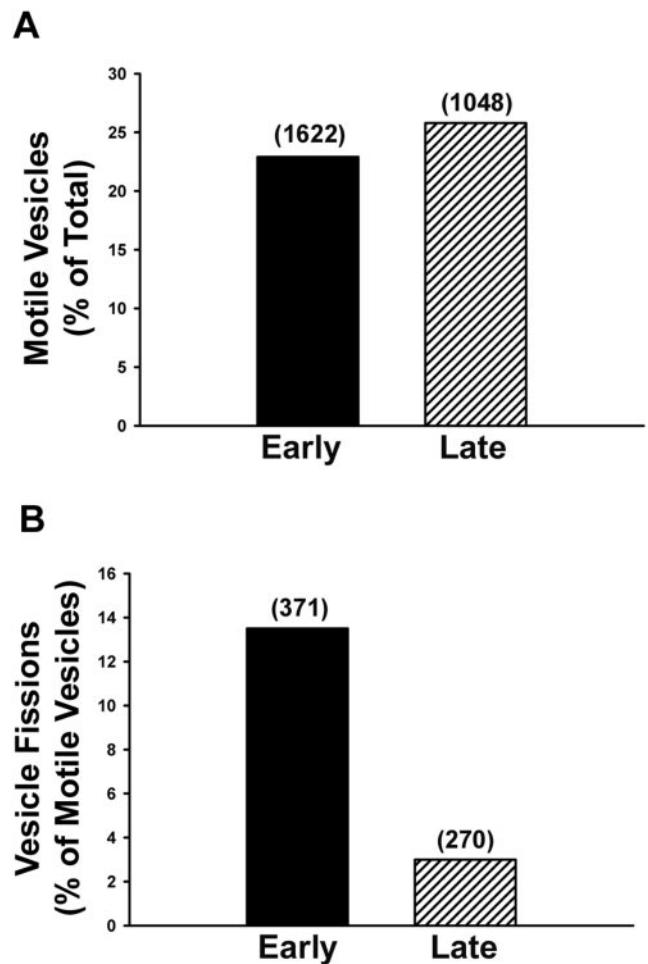

Figure 4. Microtubule-based motility and fission of early and late endocytic vesicles. Texas-red–labeled early and late endocytic vesicles were bound to rhodamine-labeled microtubules (MTs) within a glass microscopy chamber. Motility (A) and fission (B) of these vesicles were quantified following addition of 50 μM ATP. The total number of MT-bound vesicles and the total number of motile vesicles that were examined are shown in parentheses in A and B, respectively.

1995; Burkhardt *et al.,* 1997; Valetti *et al.,* 1999; Allan and Schroer, 1999). In the present study, we examined the effect of preincubation of early and late endocytic vesicles with anti-dynamitin IgG on their binding to MTs (Figure 8A). As seen in Figure 8A, this had no effect on the number of early endocytic vesicles that were attached to MTs. In contrast, dynamitin antibody preincubation resulted in a 65% reduction in the number of MT-bound late endocytic vesicles. Motor proteins associated with late endocytic vesicles that bound to MTs after preincubation with dynamitin antibody were determined (Figure 8B). Dynein was associated with only a small percentage of these vesicles. Similar results were obtained for KIF3A and KIFC2. In contrast, kinesin was associated with the majority of these vesicles, suggesting that they may represent a small population of early endocytic vesicles that is mixed in with the larger population of late endocytic vesicles.

Purification of Alexa 488-ASOR–containing Endocytic Vesicles

Preparation of Fluorescence-sorted Vesicle Fractions The studies presented above were performed on populations of
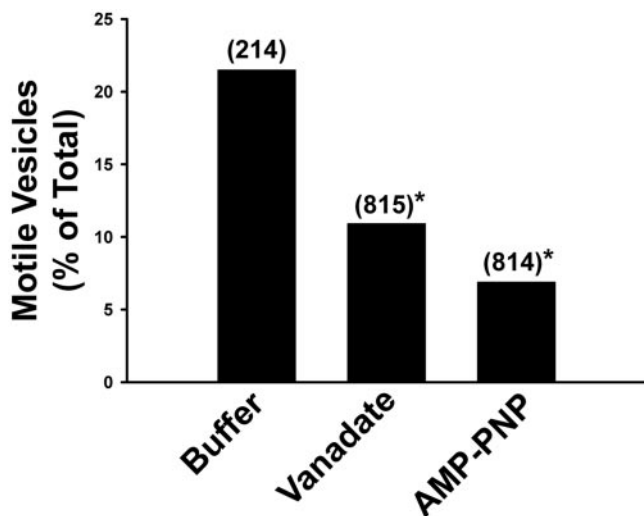
Figure 5. Effects of vanadate and AMP-PNP on motility of late endocytic vesicles. Late endocytic vesicles were perfused into the chamber and bound to MTs. The bars indicate the percentage of vesicles that moved along MTs following addition of 50 μM ATP in control buffer or in the presence of 5 μM vanadate or 1 mM AMP-PNP. The total number of vesicles examined is shown in parentheses. *p < 0.0001 compared with buffer alone.

Figure 7. Effect of specific motor antibodies on late endocytic vesicle motility. MT-bound late endocytic vesicles were incubated with antibodies to specific motor proteins, as indicated, for 6 min. Motility was then quantified after 50 μM ATP addition. The total number of MT-bound vesicles examined is shown in parentheses. *p < 0.0004 compared with buffer or nonimmune IgG.

vesicles that contained fluorescent endocytic vesicles and a substantial fraction of unlabeled vesicles. Although vesicle behavior and protein composition can be examined by microscopy-based techniques, biochemical studies performed on these mixed populations of vesicles could not be easily interpreted. To obviate this limitation, we adapted flow cytometry technology to isolate the fluorescent endocytic vesicle subpopulations. In these studies, Alexa-488 conjugated ASOR was used because of its more convenient excitation and emission characteristics. A schematic diagram of the protocol used for purification of fluorescent endocytic vesicles is shown in Fi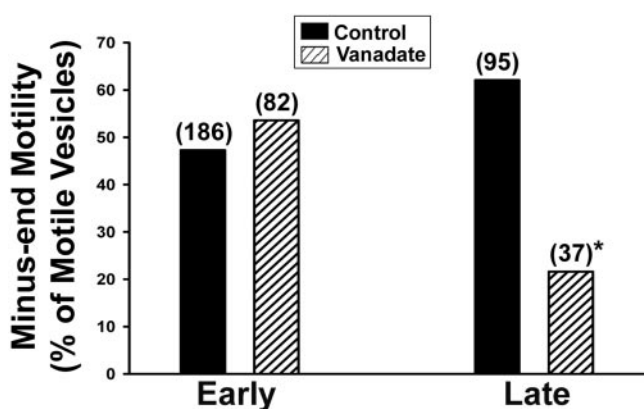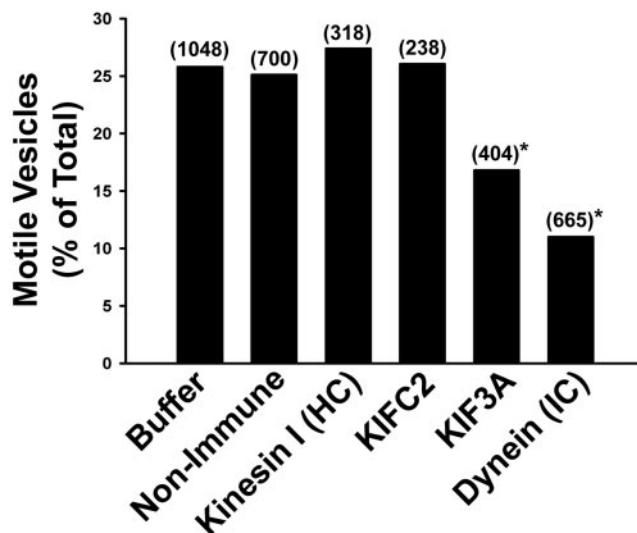gure 1. The Roman numerals in this diagram indicate the sorting parameters that were used and include doublet (I), size (II) and fluorescence (III) discrimination. The resulting vesicle fractions are indicated by lower case letters (a-h). Representative dot plots of the doublet and size discrimination data for a late fluorescent endocytic vesicle preparation are shown in Figure 9, A and B. As these data are not dependent on vesicle fluorescence, identical plots were seen for unlabeled or fluorescent endocytic vesicle preparations (unpublished data). The results of fluorescence sorting of 100,000 early or late endocytic vesicles are shown in the histograms that appear in Figure 9, C and D, respectively, and are compared with results obtained with control vesicles that were isolated from rat livers without prior injection of Alexa-488 ASOR. The distribution of control vesicles was used to set the fluorescence threshold that was specific for vesicles that contained Alexa-488 ASOR, as indicated by region (h) in each histogram.

Purity of Fluorescence-sorted Vesicle Fractions Colocalization of Alexa 488-ASOR with DiD, a fluorescent compound that nonspecifically labels membranes (Honig and Hume, 1986; Huth *et al.*, 2004), was used as a determinant of purity of sorted fluorescent endocytic vesicles. A representative study of a late endocytic vesicle preparation is shown in Figure 10. Examination of a mixed population of vesicles (Figure 1f) reveals that DiD labeled a substantial number of vesicles that did not have Alexa 488 signal (Figure 10, A and B). After sorting based upon Alexa 488 fluorescence, DiD fluorescence colocalized with ~99% of Alexa 488–containing vesicles, (Figure 10, C and D). Studies of early endocytic vesicles gave identical results (unpublished data).

Biochemical Analysis of Fluorescence-sorted Vesicle Fractions Localization of specific proteins to sorted vesicle populations was determined by immunoblot. As seen in Figure 11A, all of the proteins that were examined were detected in the starting vesicle populations before sorting (Figure 1a). Examination of presorted vesicles that were prepared from

Figure 6. Directional motility of early and late endocytic vesicles. Polarity-marked MTs were prepared and bound to the inner surface of a glass microscopy chamber. Early or late endocytic vesicles were then perfused into the chamber and bound to MTs. The bars indicate the percentage of early (left) and late (right) endocytic vesicles that moved toward the minus-end of MTs after addition of 50 μM ATP in the presence or absence of 5 μM vanadate. The total number of motile vesicles examined is shown in parentheses. *p < 0.002 compared with control late vesicles.

Table 1. Effect of guanosine nucleotide analogues on MT-based motility and fission of late endocytic vesicles

Nucleotide	No. of experiments	Total no. of fluorescent vesicles	No. of motile fluorescent vesicles (% of total)	No. of motile fluorescent vesicles undergoing fission (%)
None	4	457	146 (32%)	6 (4%)
GTP-γ-S	4	531	173 (33%)	5 (3%)
GDP	5	614	198 (32%)	4 (2%)

MT-bound Texas-Red-ASOR–containing late endocytic vesicles were incubated for 5 min in a motility chamber with buffer alone or with buffer containing 4 mM GTP-γ-S or GDP. Motility of late endocytic vesicles and fission of motile vesicles were monitored after addition of 100 μM ATP.

rat livers 5 or 15 min after injection of Alexa 488-ASOR had identical levels of these proteins and total protein concentrations (unpublished data). After sorting, as seen in Figure 11A, the fluorescent early endocytic vesicles, were highly associated with the ASGPR, Rab4, KIFC2, and KIF5B. Traces of KIF3A and dynactin were observed, whereas dynein, Rab5, and Rab7 were essentially absent. Sorted fluorescent late endocytic vesicles had reduced association with ASGPR and Rab4. Rab5 and KIF5B were absent but there was substantial association with KIFC2, KIF3A, Rab7, dynactin, and dynein. These results are in agreement with those obtained by immunofluorescence of MT-bound vesicles (Figure 3).

As seen in Figure 11B, ASGPR and Rab4, deenriched in fluorescent late endocytic vesicles, were recovered in the unlabeled vesicle fraction, corresponding to panel g of Figure 1. Interestingly, although Rab5 was easily detectable in both early and late presorted vesicle preparations (Figure 1a), its recovery in the sorted fluorescent (Figure 1h) or unlabeled (Figure 1g) fractions was low (Figure 11B). This could be due to degradation or loss of this protein from vesicles. To determine the fate of Rab5 during the purification procedure, vesicles that would normally have been discarded, namely aggregated vesicles (Figure 1b) and small vesicles (Figure 1d), were collected and analyzed. As seen in Figure 11B, Rab5 was present in the small, but not in the aggregated vesicle fraction. ASGPR and Rab4 were detected in both of these fractions.

DISCUSSION

In previous studies, we prepared a mixed population of vesicles from rat liver 5 min after portal venous injection of Texas-red-ASOR (Bananis *et al.,* 2000; Murray *et al.,* 2000).

Because the resulting fluorescent vesicles contained both ligand (ASOR) and receptor (ASGPR; Bananis *et al.,* 2000, 2003), we concluded that they represented a population of presegregation early endocytic vesicles. Using a cell-free fluorescence microscopy-based system, motility and fission of these vesicles on MTs were reconstituted and shown to depend on plus- and minus-end–directed kinesin motors, but not dynein (Bananis *et al.,* 2000, 2003; Murray *et al.,* 2002). We also showed that conversion of Rab4-GTP to Rab4-GDP was associated with the activation of the minus-end kinesin, KIFC2, that was bound to these early endocytic vesicles. Rab5, which is generally thought to be a constituent of early endocytic vesicles, was absent (Bananis *et al.,* 2003).

The present report extends these studies to characterization of endocytic vesicles prepared from rat liver 15 min after portal venous injection of fluorescently labeled ASOR. As compared with early ASOR-containing endocytic vesicles, these fluorescent vesicles had little association with the ASGPR (Figures 2 and 3). These ligand-containing, receptor-depleted vesicles did not undergo fission (Figure 4), consistent with their characterization as postsegregation late endocytic vesicles (Schmid *et al.,* 1988; Stoorvogel *et al.,* 1991; Casciola-Rosen *et al.,* 1992; Dunn and Maxfield, 1992). In contrast to early endocytic vesicles, these late vesicles were substantially associated with dynein, dynactin, KIF3A, KIFC2, and Rab7, a known late endocytic vesicle marker (Feng *et al.,* 1995; Meresse *et al.,* 1995; Lebrand *et al.,* 2002). They had little association with Rab4 or conventional kinesin I, two proteins that we found associated with early endocytic vesicles (Bananis *et al.,* 2003).

Several previous studies suggested that dynein plays a role in motility of late endocytic vesicles (Oda *et al.,* 1995; Pol *et al.,* 1997; Valetti *et al.,* 1999; Jordens *et al.,* 2001; Lebrand *et*

Figure 8. Effect of preincubation with dynamitin antibody on attachment of endocytic vesicles to MTs. Endocytic vesicles were preincubated with mAb to dynamitin (p50 subunit of dynactin complex) or nonimmune mouse IgG (control) for 6 min. After incubation, vesicles were perfused into MT-coated glass microscopy chambers. (A) The bars indicate the number of fluorescent vesicles that bound per μm microtubule length. Results shown are mean and SD. (B) Immunofluorescence localization of the indicated proteins on MT-attached late endocytic vesicles with or without preincubation with antidynamitin antibody. The total number of MT-bound vesicles examined for each experiment is shown in parentheses. *$p < 0.0001$ compared with each control.
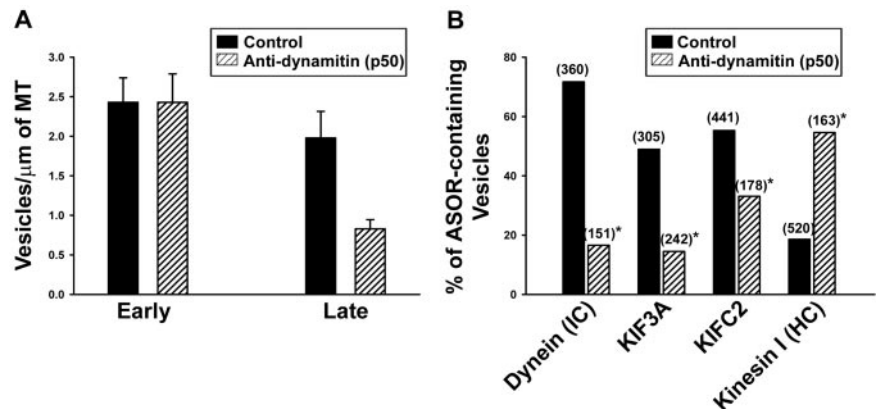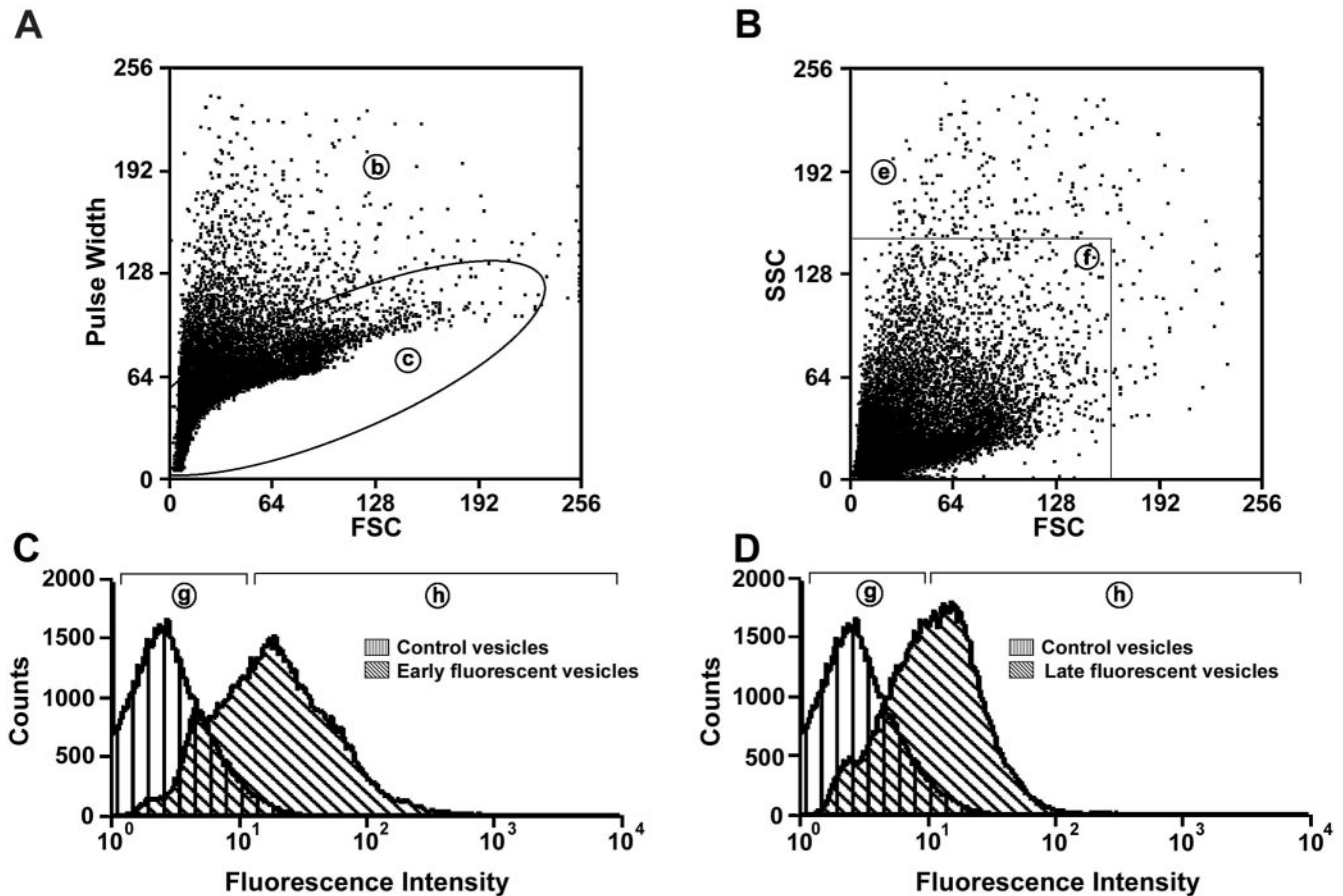
Figure 9. Flow cytometric analysis and purification of fluorescent endocytic vesicles. Alexa 488–labeled endocytic vesicles were prepared and sorted on a Dykocytomation (MoFLo) Cell Sorter. Regions indicated by lower case letters in circles in this figure correspond to those indicated schematically in Figure 1. (A) Dot plot representation of forward scatter (FSC) vs. pulse width of presorted vesicles. (B) Dot plot representation of FSC vs. side scatter (SSC) of vesicles within region (c) of dot plot (B). (C) and (D) Fluorescent profiles of unlabeled (control) or early (C) or late (D) endocytic vesicles within region (f) of dot plot (B).

al., 2002) and others have reported that motility of these vesicles is bidirectional (Rodriguez *et al.,* 1996; Santama *et al.,* 1998; Wubbolts *et al.,* 1999). The present studies directly demonstrate that motility of late endocytic vesicles is mediated by dynein (minus-end) and KIF3A (plus-end). Motility is inhibited by antibodies specific to these motors, but not by antibodies to conventional kinesin I or KIFC2 (Figure 7) that inhibit motility of early endocytic vesicles (Bananis *et al.,* 2000, 2003). The present results are in agreement with recent studies that showed that KIF3A (kinesin II) and dynein bound to dynactin and mediated bidirectional motility of *Xenopus laevis* melanophores along MTs (Deacon *et al.,* 2003). We showed that preincubation of endocytic vesicles with dynamitin antibody prevented the binding of dynein-associated vesicles to MTs (Figure 8A). The mechanism for this effect is unknown, but could result from antibody-mediated disruption or steric hindrance of proteins comprising the dynactin complex. Vesicles that were able to bind to MTs after dynamitin antibody incubation had significantly reduced association with dynein, KIF3A and KIFC2, but were highly associated with conventional kinesin I (Figure 8B).

The functional significance of the association of the minus-end–directed kinesin, KIFC2, with late endocytic vesicles is not clear. In contrast to results with early endocytic vesicles (Bananis *et al.,* 2003), antibody to KIFC2 does not affect motility of late endocytic vesicles (Figure 7). The functional

consequences of the plus-end–directed kinesin, KIF3A, being present on late endocytic vesicles is not yet known. Recent studies showed that KIF3A was required for insulin-induced GLUT4-containing exocytic vesicles to traffic to the surface of adipocytes (Imamura *et al.,* 2003). In addition, a number of transmembrane proteins such as cation-independent mannose-6-phosphate receptor (CI-MPR), furin, and TGN38 traffic between late endosomes and the *trans*-Golgi network and are then transported to the plasma membrane (Maxfield and McGraw, 2004). Other studies suggested that plus-end–directed movement of late endocytic vesicles is required for transport of LDL-derived cholesterol back to the plasma membrane (Mukherjee and Maxfield, 2000; Lebrand *et al.,* 2002). A defect within this pathway could result in accumulation of cholesterol and other lipids within late vesicle compartments, as observed in a number of cholesterol storage diseases, such as Niemann-Pick type C (Liscum and Klansek, 1998; Mukherjee and Maxfield, 2000; Lebrand *et al.,* 2002).

These morphologically based results were validated with fluorescent ligand-containing endocytic vesicles that were purified using flow cytometry–based methodology. Although others have used flow cytometry to purify vesicles (Fialka *et al.,* 1999; Pasquali *et al.,* 1999), details of the procedures and purity of resulting fractions have not been reported. The purification technology reported here should
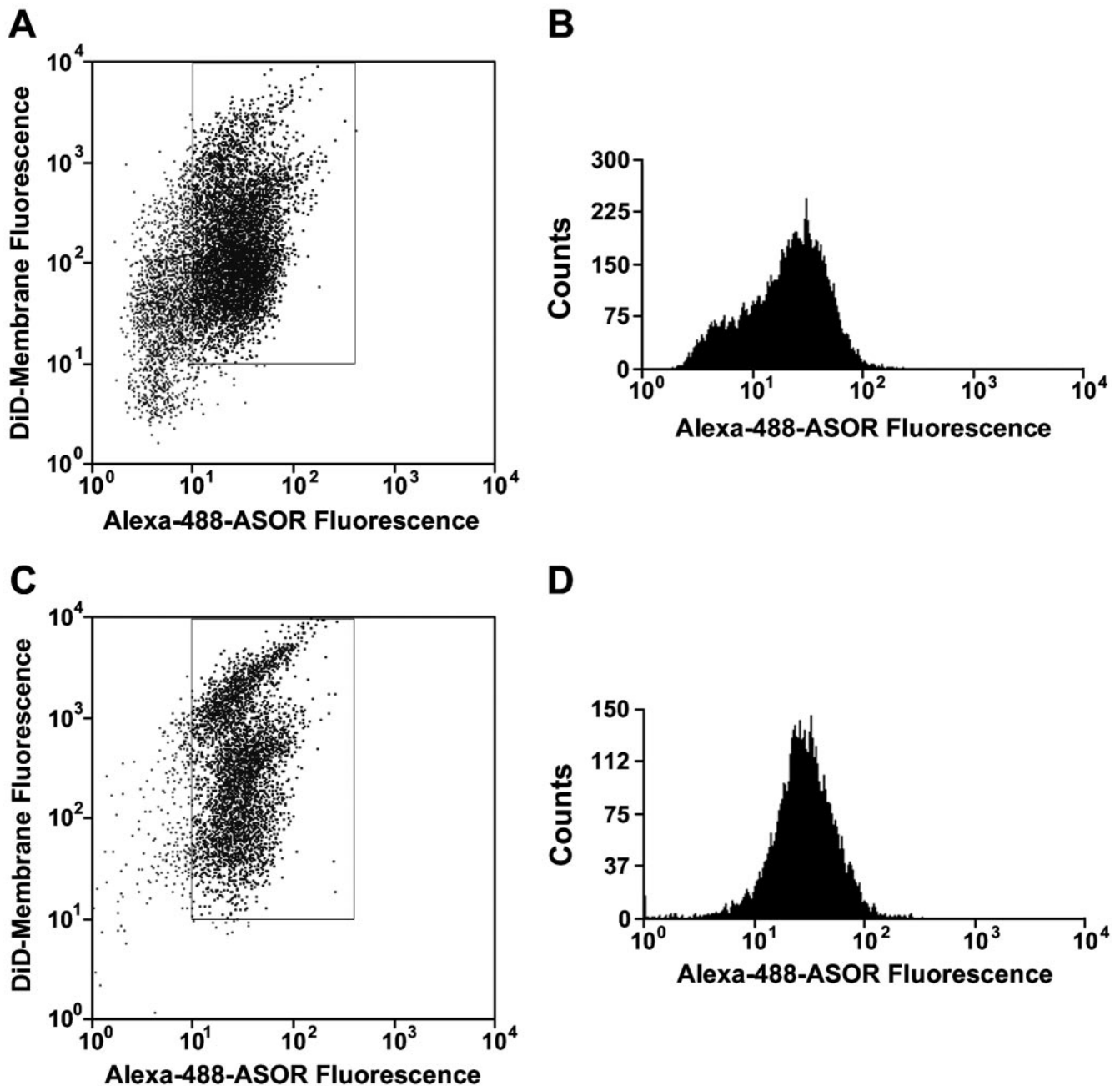
Figure 10. Flow cytometric analysis of purified vesicles colabeled with DiD. Presorted vesicles were incubated with DiD, a fluorescent general membrane marker. (A) Mixed fluorescent and nonfluorescent vesicles from region (f) in Figure 9B were analyzed for Alexa 488 and DiD fluorescence. The boxed area depicts vesicles that have both fluorescent membrane dye and fluorescent ASOR and represents 60% of total vesicles. (B) The Alexa 488 fluorescence profile of the total population of vesicles from A is shown. (C) Sorted fluorescent vesicles from region (h) in Figure 9D were analyzed for Alexa 488 and DiD fluorescence. Ninety-nine percent of total vesicles were within the boxed area. (D) The Alexa 488 fluorescence profile of the total population of vesicles from C is shown.

eventually prove highly useful for detailed proteomic analysis of proteins that comprise these vesicle populations. Our current studies show that early and late fluorescent endocytic vesicles associate with different cohorts of motor and accessory proteins. The mechanisms by which these proteins are acquired and exchanged by endocytic vesicles as they mature, remain to be fully elucidated. Although, Rab5 is thought to be a characteristic component of early endocytic vesicles (Bucci *et al.*, 1992; Gruenberg, 2001; Zerial and McBride, 2001; Stein *et al.*, 2003), it was not present on early endocytic vesicles in our preparations, but was seen associated with nonfluorescent vesicles (Bananis *et al.*, 2003). Using fluorescence-sorted vesicle fractions, we now show by immunoblot that Rab5 is found only within a fraction comprised of small vesicles that are below the size detection limit of the sorter (Figure 11). Rab4 and the ASGPR are also components of this fraction, and we hypothesize that it is composed of very early endocytic vesicles that have not yet fused following scission from the plasma membrane (Clague, 1998; Mohrmann and van der Sluijs, 1999; Rodman
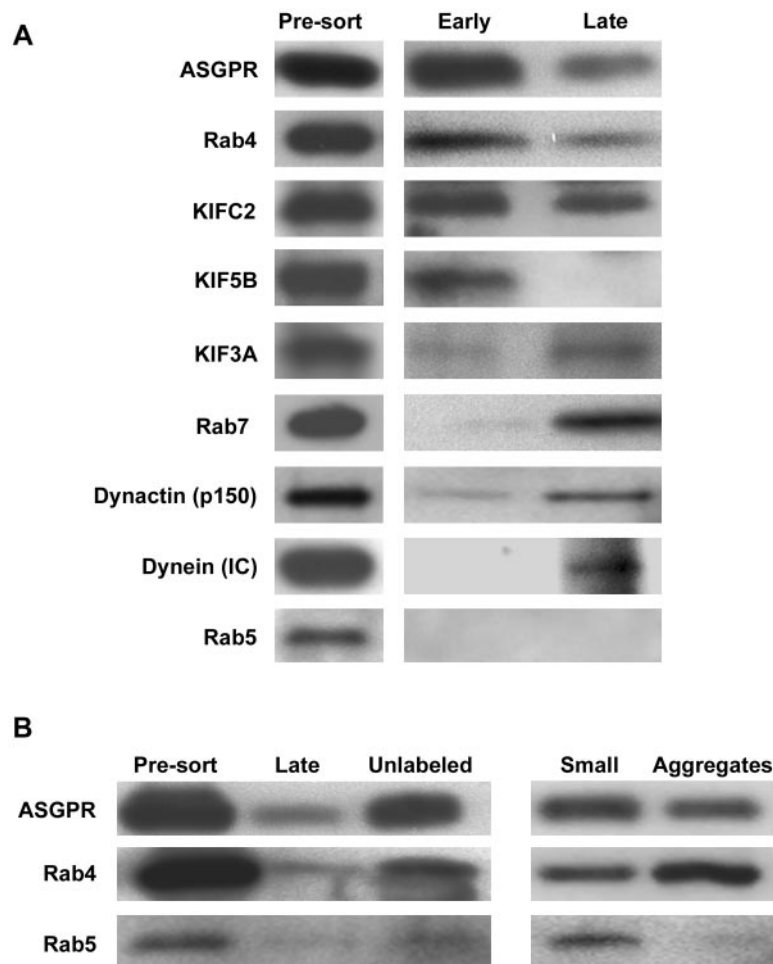
Figure 11. Immunoblot analysis of early and late endocytic vesicle populations after flow cytometric purification. Immunoblots were performed after 10–20% gradient SDS-PAGE (8 μg of protein per lane). (A) Presorted vesicles (Figure 1a) and sorted fluorescent early and late endocytic vesicles (Figure 1h) were examined for the presence of the indicated proteins. Results of a representative experiment are shown. (B) Presorted (Figure 1a), fluorescent (late) (Figure 1h), unlabeled (Figure 1g), small (Figure 1d) and aggregated (Figure 1b) late endocytic vesicles were subjected to immunoblot analysis for the ASGPR, Rab4, and Rab5 as indicated.

and Wandinger-Ness, 2000; Mousavi *et al.*, 2004). These data are consistent with the suggestion that the fluorescent pre-segregation endocytic vesicles in our preparations represent early vesicles that have passed through a transient stage in which Rab5 was bound and subsequently released.

REFERENCES

Allan, V.J., and Schroer, T.A. (1999). Membrane motors. Curr Opin. Cell Biol. *11*, 476–482.

Aniento, F., Emans, N., Griffiths, G., and Gruenberg, J. (1993). Cytoplasmic dynein-dependent vesicular transport from early to late endosomes. J. Cell Biol. *123*, 1373–1387.

Bananis, E., Murray, J.W., Stockert, R.J., Satir, P., and Wolkoff, A.W. (2000). Microtubule and motor-dependent endocytic vesicle sorting in vitro. J. Cell Biol. *151*, 179–186.

Bananis, E., Murray, J.W., Stockert, R.J., Satir, P., and Wolkoff, A.W. (2003). Regulation of early endocytic vesicle motility and fission in a reconstituted system. J. Cell Sci. *116*, 2749–2761.

Bucci, C., Parton, R.G., Mather, I.H., Stunnenberg, H., Simons, K., Hoflack, B., and Zerial, M. (1992). The small GTPase rab5 functions as a regulatory factor in the early endocytic pathway. Cell *70*, 715–728.

Burkhardt, J.K., Echeverri, C.J., Nilsson, T., and Vallee, R.B. (1997). Overexpression of the dynamitin (p50) subunit of the dynactin complex disrupts

dynein-dependent maintenance of membrane organelle distribution. J. Cell Biol. *139*, 469–484.

Casciola-Rosen, L.A., Renfrew, C.A., and Hubbard, A.L. (1992). Lumenal labeling of rat hepatocyte endocytic compartments. Distribution of several acid hydrolases and membrane receptors. J. Biol. Chem. *267*, 11856–11864.

Clague, M.J. (1998). Molecular aspects of the endocytic pathway. Biochem. J. *336*(Pt 2), 271–282.

Deacon, S.W., Serpinskaya, A.S., Vaughan, P.S., Lopez, F.M., Vernos, I., Vaughan, K.T., and Gelfand, V.I. (2003). Dynactin is required for bidirectional organelle transport. J. Cell Biol. *160*, 297–301.

Dunn, K.W., and Maxfield, F.R. (1992). Delivery of ligands from sorting endosomes to late endosomes occurs by maturation of sorting endosomes. J. Cell Biol. *117*, 301–310.

Feng, Y., Press, B., and Wandinger-Ness, A. (1995). Rab 7, an important regulator of late endocytic membrane traffic. J. Cell Biol. *131*, 1435–1452.

Fialka, I. *et al.* (1999). Identification of syntenin as a protein of the apical early endocytic compartment in Madin-Darby canine kidney cells. J. Biol. Chem. *274*, 26233–26239.

Fullerton, A.T., Bau, M.-Y., Conrad, P.A., and Bloom, G.S. (1998). In vitro reconstitution of microtubule plus end-directed, GTPγS-sensitive motility of Golgi membranes. Mol. Biol. Cell *9*, 2699–2714.

Gruenberg, J. (2001). The endocytic pathway: a mosaic of domains. Nat. Rev. Mol. Cell Biol. *2*, 721–730.

Honig, M.G., and Hume, R.I. (1986). Fluorescent carbocyanine dyes allow living neurons of identified origin to be studied in long-term cultures. J. Cell Biol. *103*, 171–187.

Huth, U., Wieschollek, A., Garini, Y., Schubert, R., and Peschka-Suss, R. (2004). Fourier transformed spectral bio-imaging for studying the intracellular fate of liposomes. Cytometry *57A*, 10–21.

Imamura, T., Huang, J., Usui, I., Satoh, H., Bever, J., and Olefsky, J.M. (2003). Insulin-induced GLUT4 translocation involves protein kinase C-lambda-mediated functional coupling between Rab4 and the motor protein kinesin. Mol. Cell Biol. 23, 4892–4900.

Jordens, I., Fernandez-Borja, M., Marsman, M., Dusseljee, S., Janssen, L., Calafat, J., Janssen, H., Wubbolts, R., and Neefjes, J. (2001). The Rab7 effector protein RILP controls lysosomal transport by inducing the recruitment of dynein-dynactin motors. Curr. Biol. 11, 1680–1685.

Karki, S., and Holzbaur, E.L. (1995). Affinity chromatography demonstrates a direct binding between cytoplasmic dynein and the dynactin complex. J. Biol. Chem. 270, 28806–28811.

Kobayashi, T., Martensen, T., Nath, J., and Flavin, M. (1978). Inhibition of dynein ATPase by vanadate, and its possible use as a probe for the role of dynein in cytoplasmic motility. Biochem. Biophys. Res. Commun. 81, 1313–1318.

Lebrand, C., Corti, M., Goodson, H., Cosson, P., Cavalli, V., Mayran, N., Faure, J., and Gruenberg, J. (2002). Late endosome motility depends on lipids via the small GTPase Rab7. EMBO J. 21, 1289–1300.

Liscum, L., and Klansek, J.J. (1998). Niemann-Pick disease type C. Curr. Opin. Lipidol. 9, 131–135.

Maxfield, F.R., and McGraw, T.E. (2004). Endocytic recycling. Nat. Rev. Mol. Cell Biol. 5, 121–132.

Mellman, I. (1996). Endocytosis and molecular sorting. Annu. Rev. Cell Dev. Biol. 12, 575–625.

Meresse, S., Gorvel, J.P., and Chavrier, P. (1995). The rab7 GTPase resides on a vesicular compartment connected to lysosomes. J. Cell Sci. 108(Pt 11), 3349–3358.

Mohrmann, K., and van der Sluijs, P. (1999). Regulation of membrane transport through the endocytic pathway by rab GTPases. Mol. Membr. Biol. 16, 81–87.

Mousavi, S.A., Malerod, L., Berg, T., and Kjeken, R. (2004). Clathrin-dependent endocytosis. Biochem. J. 377, 1–16.

Mukherjee, S., Ghosh, R.N., and Maxfield, F.R. (1997). Endocytosis. Physiol. Rev. 77, 759–803.

Mukherjee, S., and Maxfield, F.R. (2000). Role of membrane organization and membrane domains in endocytic lipid trafficking. Traffic 1, 203–211.

Murray, J.W., Bananis, E., and Wolkoff, A.W. (2002). Immunofluorescence microchamber technique for characterizing isolated organelles. Anal. Biochem. 305, 55–67.

Murray, J.W., Bananis, E., and Wolkoff, A.W. (2000). Reconstitution of ATP-dependent movement of endocytic vesicles along microtubules in vitro: an oscillatory bidirectional process. Mol. Biol. Cell 11, 419–433.

Murray, J.W., and Wolkoff, A.W. (2003). Roles of the cytoskeleton and motor proteins in endocytic sorting. Adv. Drug Deliv. Rev. 55, 1385–1403.

Novikoff, P.M., Cammer, M., Tao, L., Oda, H., Stockert, R.J., Wolkoff, A.W., and Satir, P. (1996). Three-dimensional organization of rat hepatocyte cytoskeleton: relation to the asialoglycoprotein endocytosis pathway. J. Cell Sci. 109, 21–32.

Oda, H., Stockert, R.J., Collins, C., Wang, H., Novikoff, P.M., Satir, P., and Wolkoff, A.W. (1995). Interaction of the microtubule cytoskeleton with endo-cytic vesicles and cytoplasmic dynein in cultured rat hepatocytes. J. Biol. Chem. 270, 15242–15249.

Pasquali, C., Fialka, I., and Huber, L.A. (1999). Subcellular fractionation, electromigration analysis and mapping of organelles. J. Chromatogr. B Biomed. Sci. Appl. 722, 89–102.

Pol, A., Ortega, D., and Enrich, C. (1997). Identification of cytoskeleton-associated proteins in isolated rat liver endosomes. Biochem. J. 327, 741–746.

Rodman, J.S., and Wandinger-Ness, A. (2000). Rab GTPases coordinate endocytosis. J. Cell Sci. 113, 183–192.

Rodriguez, A., Samoff, E., Rioult, M.G., Chung, A., and Andrews, N.W. (1996). Host cell invasion by trypanosomes requires lysosomes and microtubule/kinesin-mediated transport. J. Cell Biol. 134, 349–362.

Santama, N., Krijnse-Locker, J., Griffiths, G., Noda, Y., Hirokawa, N., and Dotti, C.G. (1998). KIF2beta, a new kinesin superfamily protein in non-neuronal cells, is associated with lysosomes and may be implicated in their centrifugal translocation. EMBO J. 17, 5855–5867.

Schmid, S.L., Fuchs, R., Male, P., and Mellman, I. (1988). Two distinct sub-populations of endosomes involved in membrane recycling and transport to lysosomes. Cell 52, 73–83.

Stein, M.P., Dong, J., and Wandinger-Ness, A. (2003). Rab proteins and endocytic trafficking: potential targets for therapeutic intervention. Adv. Drug Deliv. Rev. 55, 1421–1437.

Stockert, R.J. (1995). The Asialoglycoprotein Receptor: Relationships Between Struct. Funct. Express. Physiol. Rev. 75, 591–609.

Stockert, R.J., Haimes, H.B., Morell, A.G., Novikoff, P.M., Novikoff, A.B., Quintana, N., and Sternlieb, I. (1980). Endocytosis of asialoglycoprotein-enzyme conjugates by hepatocytes. Lab. Invest. 43, 556–563.

Stoorvogel, W., Strous, G.J., Geuze, H.J., Oorschot, V., and Schwartz, A.L. (1991). Late endosomes derive from early endosomes by maturation. Cell 65, 417–427.

Vale, R.D., Malik, F., and Brown, D. (1992). Directional instability of micro-tubule transport in the presence of kinesin and dynein, two opposite polarity motor proteins. J. Cell Biol. 119, 1589–1596.

Valetti, C., Wetzel, D., Schrader, M., Hasbani, M.J., Gill, S.R., Kreis, T.E., and Schroer, T.A. (1999). Role of dynactin in endocytic traffic: effects of dynamitin overexpression and colocalization with CLIP-170. Mol. Biol. Cell 10, 4107–4120.

Wersto, R.P., Chrest, F.J., Leary, J.F., Morris, C., Stetler-Stevenson, M.A., and Gabrielson, E. (2001). Doublet discrimination in DNA cell-cycle analysis. Cytometry 46, 296–306.

Wolkoff, A.W., Klausner, R.D., Ashwell, G., and Harford, J. (1984). Intracellular segregation of asialoglycoproteins and their receptor: A prelysosomal event subsequent to dissociation of the ligand-receptor complex. J. Cell Biol. 98, 375–381.

Wubbolts, R., Fernandez-Borja, M., Jordens, I., Reits, E., Dusseljee, S., Echeverri, C., Vallee, R.B., and Neefjes, J. (1999). Opposing motor activities of dynein and kinesin determine retention and transport of MHC class II-containing compartments. J. Cell Sci. 112(Pt 6), 785–795.

Zerial, M., and McBride, H. (2001). Rab proteins as membrane organizers. Nat. Rev. Mol. Cell Biol. 2, 107–117.